

Practical Channel Splicing using OFDM Waveforms for Joint Communication and Sensing in the IoT

Sigrid Dimce*, Anatolij Zubow*, Alireza Bayesteh[†],
Giuseppe Caire[‡], and Falko Dressler*

* Telecommunication Networks, TU Berlin, Germany

[†] Huawei, Canada

[‡] Communications and Information Theory, TU Berlin, Germany

{dimce, zubow, dressler}@tkn.tu-berlin.de, alireza.bayesteh@huawei.com,
caire@tu-berlin.de

Abstract—Channel splicing is a rather new and very promising concept. It allows to realize a wideband channel sounder by combining multiple narrow-band measurements. Among others, channel splicing is a sparse sensing techniques suggested for use in joint communication and sensing (JCAS), channel measurements and prediction using cheap hardware that cannot measure wideband channels directly such as in the internet of things (IoT). This work validates the practicality of a channel splicing technique by integrating it into an OFDM-based IEEE 802.11ac system, which we consider representative for many IoT solutions. Our system allows computing both the channel impulse response (CIR) and the channel frequency response (CFR). In this paper, we concentrate on the impact of the number of sub-bands in our study and show that even using only 50% of the overall spectrum leads to very accurate CIR measures. We validate the system in simulation and confirm the results in an experimental in-door scenario using software defined radios.

Index Terms—Joint communication and sensing, JCAS, channel sounder, channel splicing, internet of things, IoT

I. INTRODUCTION

Joint communication and sensing (JCAS) is becoming more important in different application domains, both in 6G as well as for the internet of things (IoT) [1]–[4]. This also triggered an ongoing discussion of appropriate waveforms, orthogonal time frequency space (OTFS) being considered a possible compromise [5]. However, most existing communication systems are based on orthogonal frequency division multiplexing (OFDM), so, integrating sensing here is very important [6].

Channel sounding is the core functionality required for JCAS, but also for channel estimation and channel prediction techniques. For example, commodity WiFi devices have been used for purposes other than wireless communication such as indoor localization and channel sounding due to the relatively low cost [7], [8]. Channel sounding relies on the channel state information (CSI) of the communication link. In case of a single-antenna device, the CSI is equivalent to the channel frequency response (CFR), which provides channel information in the frequency domain. Through Fourier transformation, the channel is characterized in the delay domain, represented by the channel impulse response (CIR). The CIR describes the multipath channel over the delay domain. However, the accuracy of the estimated CIR is limited by the channel bandwidth (BW) supported by the system. Precise measurement

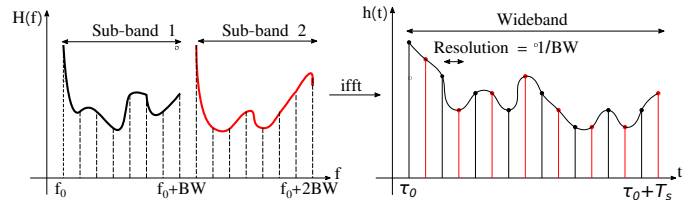


Figure 1. Illustration of the channel splicing concept

of multipath components is only possible using wideband signals. In the delay domain, the resolution is equal to $1/BW$, which, multiplied with the speed of light, gives the necessary difference between the distance of two distinct paths. For instance, a bandwidth of 20 MHz implies that the distance traveled by the signal from two distinct paths should have at least a difference of 15 m, so that the paths are distinguishable at the receiver [8].

However, in general, wideband sounding is quite complex and energy inefficient for existing communication systems. Also, many IoT systems can only process narrow-band subchannels. A possible solution to this issue is given by multi-band sensing or spectrum splicing [9]. Conceptually, channel splicing means measuring multiple narrow-band sub-bands/subchannels and then combining the results to obtain, ideally, the same results as generated by a single wideband measurement. The concept is depicted in Figure 1.

Initially, spectrum splicing was developed targeting indoor localization applications [8], [10], [11], and later extended to other applications such as human sensing [12]. This technique allows a single WiFi device to transmit packets and extract CSI in the multiple frequency bands tens of megahertz wide. The collected information through multiple bands is combined mimicking a wideband channel. Channel splicing exploits the sparse nature of the CIR and applies sparse recovery method on the collected data to obtain CIR with high resolution. The delay associated with the shortest path enables estimating the signal time of flight (ToF), which is used for localization. As we will demonstrate in this paper, splicing can also be performed on a subset of the sub-bands with only small reduction in accuracy. Despite its advantages, splicing faces several challenges due to transceiver impairments.

A few algorithms have been developed aiming to enhance the splicing performance and resolve the impairments challenges [7]–[11], [13]. Our work builds upon the theoretical concepts of spectrum splicing presented in [8]. We first implement a communication system in MATLAB based on the IEEE 802.11ac standard. We perform channel estimation based on the least square (LS) estimation technique both in time and frequency domain. We extended the system by spectrum splicing allowing to combine CFR measurements from multiple bands. The channel sounder utilizes software defined radio (SDR) components, we used two USRP N310 in the lab, for transmitting/receiving the signal over the air. We validate the practical use of splicing technique in simulations and indoor experiments by splitting a wide channel bandwidth into narrower bands, collect the CFR over these bands, perform splicing on the collected data and compare the estimated CIR with the wide channel. Our results build the basis for OFDM-based JCAS solutions and for low-cost IoT channel sounding.

Our main contributions can be summarized as follows:

- We implement a practical OFDM communication system based on IEEE 802.11ac and the LS estimation technique on the receiver to compute both CIR and CFR.
- We extend the system by incorporating the spectrum splicing to investigate the impact of the number of sub-bands, and the accuracy of the sensing approach.
- We validate the splicing technique in a controlled simulation environment as well as in a set of indoor experiments focusing on the numbers of multipath component.

II. RELATED WORK

Channel sounding is a crucial technique for generating knowledge to characterize the wireless channel in a certain frequency band. The principle of sounding is to transmit a known baseband signal up-converted at the frequency of interest, which is post-processed on the receiver side for extracting metrics (CIR, CFR) that provide channel information. Several sounding techniques were developed over the years with the sole purpose to accurately characterize the propagation channel. The two most common techniques are the spread spectrum sliding correlator [14] and the OFDM-based system [15]. Both techniques have demonstrated undeniable success at lower frequencies, as well as at millimeter-wave (mmWave) frequency band [16], [17]. The OFDM-based system consists of multiple subcarriers, where each subcarrier sees the channel as flat, hence, allowing it to overcome the main drawback of wideband transmission in terms of frequency selectivity. Nevertheless, the system requires a large peak-to-average-power ratio (PAPR) as well as tight receiver synchronization. On the other hand, the spread spectrum sliding correlator “spreads” the carrier signal over a large bandwidth by mixing it with a binary PN sequence. The received signal is mixed with a slower identical version of the PN sequence, which makes the system less vulnerable towards interference, but more complex in terms of hardware and software implementation compared to the OFDM system. Thus, choosing one of the aforemen-

tioned sounding techniques is application specific and requires to compromise between robustness and complexity.

Propagation information is provided in the delay and frequency domain, respectively, CIR and CFR, which are computed by the channel estimation techniques. Among the existing ones, the LS estimation is the most common method characterized by low computational complexity. Yet, in a few application scenarios, this technique yields inferior performance [18]. Another well-known estimation method is the minimum mean square error (MMSE) [15], which minimizes the channel estimation error. However, MMSE leads to high computational complexity and requires prior channel statistic information, which sometimes is not available. Beside these traditional techniques, new models based on deep learning are being developed [18], targeting performance improvement, and using LS estimation for training their model.

Reducing system costs by using existing hardware infrastructure for applications such as channel sounding is becoming more crucial. In this aspect, spectrum splicing methods are attracting high attention in the recent years. Most of the existing works target indoor localization applications [7], [8], [10], [13], and a few others e.g., human sensing [12]. The developed methods aim estimating the multipath component (MPC) delays precisely considering the present of hardware distortions. For instance, Chronos [7] is an indoor positioning system, which estimates sub-nanosecond ToF using compressed sensing sparse recovery methods on the collected CFRs over multiple bands. The algorithm addresses the phase offset issue as a result of hopping between frequency bands. Splicer [11] is a software-based system that splices multiple CSIs measurements and achieves single-AP localization. The authors propose several techniques for hardware impairment corrections. The work in [13] presents a two-stage global estimation scheme, which aims to improve estimation accuracy firstly by achieving initial delay estimation based on a coarse signal model and then a global delay estimation. Other authors [10] use the shift-invariance structure in the multiband CSI and propose a weighted gridless subspace fitting algorithm for the delay estimation. The fundamental limits and optimization of multi-band splicing in terms of the time delays are analyzed and presented in [9]. The statistical resolution limit is derived for the delay resolution and an algorithm is proposed to solve the parameters optimization problem. A grid-based multi-band splicing technique is presented in [8]. The method is characterized by low-complexity and can easily scale to large-dimensional problems. Besides localization, other mechanisms, such as WiRIM [12], utilize spectrum splicing for human sensing applications.

We integrate the theoretical concepts proposed in [8] into an OFDM-based JCAS system. We validated our practical implementation of channel splicing both in simulation as well as an experimental indoor scenario.

III. SPECTRUM SPLICING ARCHITECTURE

Our channel sounder is based on the spectrum splicing technique presented in [8]. The developed method exploits the

sparse nature of the CIR and utilizes a grid-based compressed sensing technique to estimate the path delays and amplitude. On a high abstraction level, the idea is to use subchannels to reconstruct the CIR with high resolution as shown in Figure 1.

A. Spectrum Splicing Concept

The system is based on OFDM and packets are transmitted over M frequency bands, where each band is composed of N subcarriers. The subcarriers are indexed according to the integer set $\mathcal{N} = \{-\frac{N-1}{2}, \dots, \frac{N-1}{2}\}$, where N is an odd integer. The presented technique performs the estimation based on the pilot signals, which in the receiver side can be written as

$$y[m, n] = H[m, n]S_{m,n} + z[m, n], \quad m \in [M], n \in \mathcal{N} \quad (1)$$

where $S_{m,n} = 1$ is the pilot symbol transmitted over the n -th subcarrier of band m ($f_{m,n}$), which without loss of generality is assumed to be 1; $H[m, n]$ denotes the CFR in the same subcarrier, and the $z[m, n] \sim \mathcal{CN}(0, 1/\text{SNR})$ is the additive white Gaussian noise (AWGN) channel.

Assuming that the propagation environment is comprised of K scatters, the CIR over the delay domain is given as

$$h(\tau) = \sum_{k=1}^K c_k \delta(\tau - \tau_k), \quad (2)$$

where $\delta(\cdot)$ stands for Dirac's delta function, $\tau_k \in [0, 1/f_s)$ is the delay associated with each path k (f_s - subcarrier spacing), and $c_k \in \mathbb{C}$ is corresponding amplitude. The parameter of gain and delay are independent of the frequency band. On the other hand, the CFR samples are computed from the CIR via the Fourier transformation, and can be written as

$$H[m, n] = \mathcal{F}\{h(\tau)\} |_{f=f_{m,n}} = \sum_{k=1}^K c_k e^{-j2\pi f_{m,n} \tau_k}, \quad (3)$$

for $m \in [M], n \in \mathcal{N}$. Furthermore, during the transmission, the pilot samples are affected by several distortions caused by the hardware devices, which lead to the phase term

$$\psi[m, n] = -2\pi(\delta_m n f_s + \phi_m), \quad m \in [M], n \in \mathcal{N} \quad (4)$$

where $\delta_m \in [0, 1/f_s)$ stands for the timing offset due to the packet detection delay (PDD) and the sampling frequency offset (SFO), and $\phi_m \in [0, 1)$ represents the phase offset due to the carrier frequency offset (CFO) between transmitter and receiver, and the phase offset due to switching channel bands. The two parameters, δ_m, ϕ_m differ from one band to the other such that, $\psi[m, n]$ is a linear function in each band, of the subcarrier index with different slope and constant term. As a result, the received pilot samples, including the distortion component are represented in the following form

$$\begin{aligned} y[m, n] &= e^{j\psi[m,n]} H[m, n] + z[m, n] \\ &= e^{j\psi[m,n]} \sum_{k=1}^K c_k e^{-j2\pi f_{m,n} \tau_k} + z[m, n] \\ &= \sum_{k=1}^K c_k e^{-j2\pi(f_{m,0}\tau_k + \phi_m)} e^{-j2\pi n f_s (\delta_m + \tau_k)} + z[m, n] \end{aligned} \quad (5)$$

where for each band the subcarriers are assumed to be equispaced with a space equal to f_s and $f_{m,n} = f_{m,0} + n f_s, n \in \mathcal{N}$, and $f_{m,0}$ being the carrier frequency of band m .

The proposed spectrum splicing technique aims to estimate the CIR based on noisy and distorted pilot samples, using the following steps:

- 1) For each band $m \in [M]$ estimate and remove the distortion parameters δ_m, ϕ_m . The estimation is performed using the sparse recovery technique of atomic norm denoising (AND).
- 2) Splice the clean pilot data to obtain a high-resolution estimated CIR using the orthogonal matching pursuit (OMP) sparse recovery technique.
- 3) Resolve ambiguities using a hand-shaking procedure between the two communication nodes.

In this work, we focus on the second step of multi-band splicing and perform the estimation based on the very high throughput long training field (VHT-LTF) of 802.11ac frame. On the receiver side, time and CFO is estimated and corrected.

The multi-band splicing technique consists of merging the measurements conducted over several bands, increasing the resolution of the estimated CIR by expanding the measurement bandwidth. For instance, the resolution over the delay domain obtained from the measurements over a single band is given as $(\Delta\tau)_1 = 1/N f_s$, whereas over M frequencies band it increases to $(\Delta\tau)_1 = 1/MN f_s$. Considering that the CIR is sparse, the authors in [8] used compressed sensing, and more specifically the OMP sparse recovery method to recover the CIR. Firstly, a vector is defined containing the subcarriers per band $\mathbf{f}(m) = [f_{m,-(N-1)/2}, \dots, f_{m,(N-1)/2}]^T$ and for all the bands $\mathbf{f} = [\mathbf{f}(1)^T, \dots, \mathbf{f}(M)^T]^T \in \mathbb{R}^{MN}$. Similarly, a vector is defined containing the clean CFR samples per band $\tilde{\mathbf{y}}(m) = [\tilde{y}[m, -(N-1)/2], \dots, \tilde{y}[m, (N-1)/2]]^T$ and for all the bands $\tilde{\mathbf{y}} = [\tilde{\mathbf{y}}(1)^T, \dots, \tilde{\mathbf{y}}(M)^T]^T \in \mathbb{C}^{MN}$. Furthermore, the elements of the $\tilde{\mathbf{y}}$ can be written as

$$[\tilde{\mathbf{y}}]_i = \mathcal{F}\{h_0(\tau)\} |_{[f_i + \tilde{\mathbf{z}}_i]} \quad i = 1, \dots, MN \quad (6)$$

with $[\tilde{\mathbf{z}}_i]$ representing the AWGN plus the error due to the phase-distortion removal procedure. In order to apply the OMP method, a uniform grid of size G is defined over the delay domain as $\mathfrak{G} = \{0, 1/G, \dots, G-1/G\}/f_s$, and a dictionary \mathbf{D} as $\mathbf{D} = [\mathbf{d}(0), \dots, \mathbf{d}(G-1)] \in \mathbb{C}^{MN \times G}$, where $G \gg MN$ and each column $\mathbf{d}(i)$ given as

$$\mathbf{d}(i) = \frac{1}{\sqrt{MN}} [e^{-j2\pi [f_1(\frac{i}{G})/f_s]}, \dots, e^{-j2\pi [f_{MN}(\frac{i}{G})/f_s]}]^T \in \mathbb{C}^{MN}, \quad (7)$$

where $i = 0, 1, \dots, G-1$. For values of $G = 2MN$, or $G = 3MN$ the grid \mathfrak{G} is considered dense and the vector in (6) can be approximated to

$$\tilde{\mathbf{y}} \approx \mathbf{D}\mathbf{h}_0 + \tilde{\mathbf{z}} \quad (8)$$

where $\mathbf{h}_0 \in \mathbb{C}^G$ is a discrete approximation for h_0 , and is estimated using the OMP sparse recovery method and the given $\tilde{\mathbf{y}}$ samples. The OMP method is a greedy iterative algorithm, that selects a column of the dictionary \mathbf{D} , at each iteration, such that it has the highest correlation with the

current residual and it repeats until a convergence condition is met [19]. For each selected column, the non-zero coefficients are computed using the least-square method, such that they approximate the measurement vector \tilde{y} . The algorithm stops once the number of the selected dictionary columns reaches the sparsity order of \mathbf{h}_0 , which is given as input.

B. Practical Channel Splicing for OFDM Systems

In the following, we describe the system architecture and the estimation technique used for generating the CIR and CFR. The SDR-based channel sounder builds upon USRP-components to perform the over-the-air communication, and MATLAB for the software implementation.

The OFDM transmitter is implemented according to the 802.11ac standard. This standard support the signal bandwidths of 20, 40, 80 and 160 MHz. Despite the different signal bandwidths, the OFDM subcarrier spacing is kept fixed to 312.5 kHz, whereas the number of the subcarriers changes accordingly. Firstly, the transmitter converts the payload message into a sequence of bits, which later are binary phase shift keying (BPSK) and OFDM modulated. For over-the-air experiments, the generated baseband signal is forwarded to the USRP SDR, which upconverts it to the carrier frequency of interest. The connection between MATLAB and the USRP is realized through the recently released Wireless Testbench toolbox¹, which supports high-speed data transmission.

We also use preamble detector functionality provided by the toolbox, allowing capturing only the signal of interest for offline analysis. Once packets in the air are detected by the preamble detector, the signal is captured, downconverted, and the raw data is stored into a binary file for further post-processing on the host computer. During post-processing, the time and carrier frequency offset are estimated using the frame preamble and compensated per each received packet. The channel is estimated based on the VHT-LTF sequence in the preamble using the LS estimation technique, and the obtained CIR and CFR are stored. Finally, the signal is decoded and demodulated, and the transmitted payload message is recovered. The collected CFR samples over multiple narrow frequency bands are used as input to the spectrum splicing technique for estimating the wideband channel.

Channel estimation is performed using LS estimation time or frequency domain approach [15] on the VHT-LTF. The time-domain approach computes the CIR as

$$\hat{h} = X^\dagger y \quad (9)$$

where y are the received samples, \hat{h} is the CIR and X^\dagger is the Moore-Penrose (pseudo) inverse of the Toeplitz matrix X . Likewise, the frequency-domain approach acquires the CFR as

$$\hat{H} = Y./X \quad (10)$$

where Y are the received samples, \hat{H} is the CFR and the X are the transmitted samples. Both CIR and CFR can be computed

from each other using the fast Fourier transformation (FFT) and inverse FFT (IFFT).

In the following, we describe the validation of our implementation in simulation as well as results from first over-the-air experiments in an indoor scenario.

IV. PERFORMANCE EVALUATION

Channel splicing aims to estimate a wideband channel by combining multiple narrow-band channel measurements. This work validates the splicing technique presented in [8] in a controlled simulated environment and a real-world scenario, exploiting the flexibility of the developed tool to switch between theory and practice. Currently, the validation focuses only on the accuracy of the estimated delay, ignoring the amplitude, which will be analyzed in future work.

A. Simulations

Splicing is validated in simulations at the frequency band 5 GHz by splitting the wide 160 MHz bandwidth into narrower sub-bands, specifically 2×80 MHz, 4×40 MHz, and 8×20 MHz sub-bands. Simulations are run at the central frequencies listed in Table I.

The generated CFRs are combined into an array and used as input to the spectrum splicing technique. The estimated CIR is compared towards the full 160 MHz CIR obtained utilizing the LS method. In the simulated environment, we up-/down-convert to the carrier frequency of 5 GHz in software and make use of a the MATLAB Rayleigh channel. The channel model allows defining the number of the MPCs and the time delay for each path. We investigate the algorithm performance in two scenarios, and with different number of multipath components and sub-bands width.

1) *Different Frequency Resolution:* The first scenario consists of $K = 2$ MPCs, with delays and average powers set to $\{0, 18.75\}$ ns and $\{0, -2\}$ dB. The splicing technique is applied over the collected CFR samples for different sub-bands width at the corresponding center frequencies. The results are presented in Figure 2 and depicts the estimated two paths (indicated by the markers) along with the computed 160 MHz CIR. Our technique correctly estimates the two 160 MHz peaks despite the sub-channel width. In the considered scenario, the CFR samples are collected over all the sub-bands. However, we further investigate the algorithm performance, looking at only half of the sub-bands. Similarly, the results are shown in Figure 3.

As can be seen, the results for the 2×40 MHz and the 1×80 MHz show that we can correctly estimate the two strongest paths observed by the 160 MHz CIR, despite the

Table I
SIMULATION MEASUREMENT CENTER FREQUENCIES

Bandwidth	Center frequency
80 MHz	4.96, 5.04 GHz
40 MHz	4.94, 4.98, 5.02, 5.06 GHz
20 MHz	4.93, 4.95, 4.97, 4.99, 5.01, 5.03, 5.05, 5.07 GHz

¹<https://de.mathworks.com/products/wireless-testbench.html>

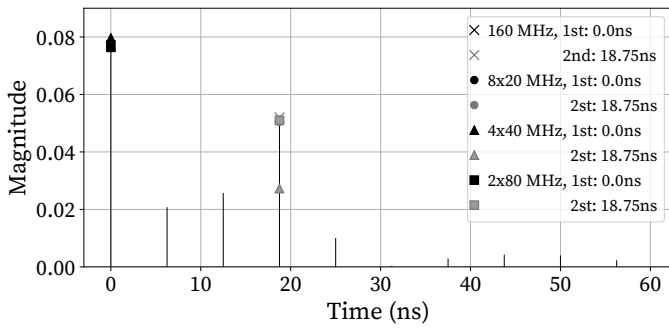


Figure 2. Estimated peaks using different sub-bands width compared towards the 160 MHz CIR.

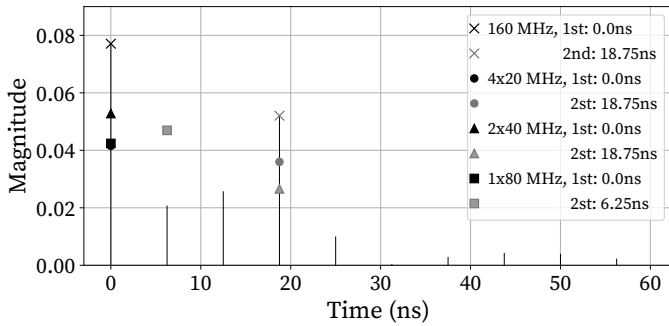


Figure 3. Estimated peaks using 50% of the sub-bands, for different sub-bands width, compared towards 160 MHz CIR.

missing samples. The results for the 4×20 MHz experiment, on the other hand, indicate that we fail estimating correctly the second path, with a difference up to 2 samples (1 sample = $1/160\text{MHz} = 6.25$ ns).

2) *Multiple Paths*: In the second scenario, we consider $K = 4$ MPCs, with delays and average powers set to $\{0, 18.75, 200, 218.75\}$ ns and $\{0, 0, -2, 0\}$ dB. Splicing is applied on CFRs samples collected over all and 50% of the 40 MHz sub-bands, with the purpose to estimate the 160 MHz CIR. The results are presented in Figure 4 and illustrate that splicing applied over all the sub-bands correctly estimate the $K = 4$ peaks delay, shown by the markers. Yet, the algorithm fails to estimate the third peak when only 50% of the sub-bands are used.

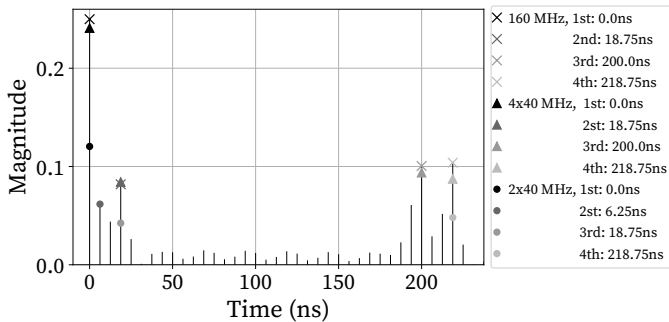


Figure 4. Estimated MPCs using spectrum splicing based on 40 MHz sub-bands for the scenario with 4 paths.

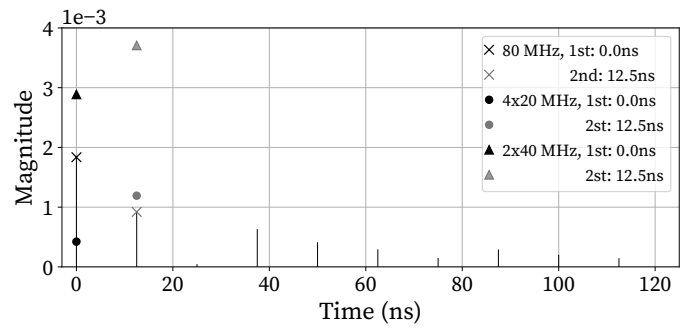


Figure 5. Estimated peaks from measurements conducted over all frequency bands and compared towards the 80 MHz CIR.

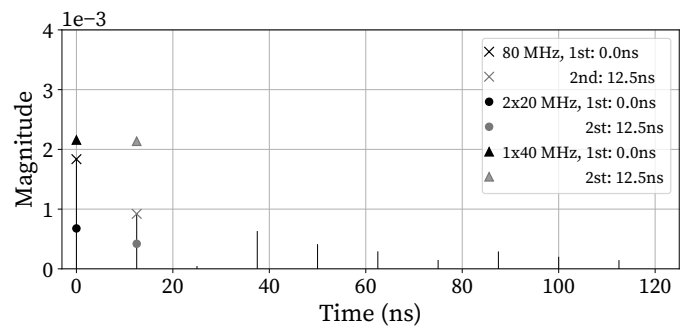


Figure 6. Estimated peaks from measurements conducted over 50% of the sub-bands and compared towards the 80 MHz CIR.

To summarize, the simulation results show that, channel splicing correctly estimates the paths delay which are distinguishable only by a wide channel, in case it is applied over the CFR samples collected over all the narrower sub-bands. The algorithm performance in some cases deteriorate when 50% of the sub-bands are utilized. As future work we aim to improve the algorithm performance when only 50% of the sub-bands are utilized which would speed up the estimation of wider channels in the range of, e.g., 1 GHz.

B. Indoor Lab-Experiments

To verify the accuracy of the spectrum splicing technique, measurements are conducted in real-world scenarios. Two USRP N310, correspondingly the transmitter and receiver, are connected through 1 Gbps Ethernet to a host computer, in which two instances of Matlab are set up. The experiments are performed indoor, at 2.4 GHz using signal bandwidth of 80 MHz and a communication distance of 4 m. Next, the wide bandwidth is divided into 2×40 MHz, 4×20 MHz sub-bands and raw data is collected at the center frequencies listed in Table II.

Table II
EXPERIMENTAL MEASUREMENT CENTER FREQUENCIES

Bandwidth	Center frequency
40 MHz	2.43, 2.47 GHz
20 MHz	2.42, 2.44, 2.46, 2.48 GHz

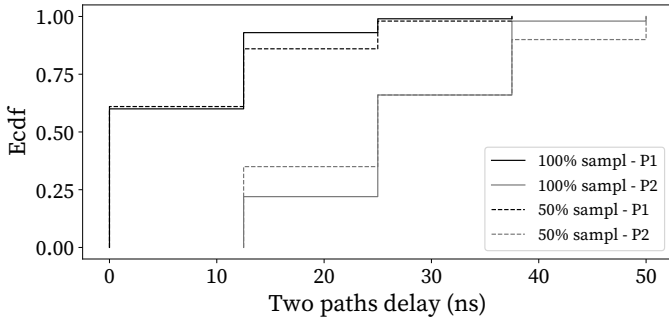


Figure 7. Computed ecdf for 2 paths estimated from splicing applied over 20 MHz sub-bands over 100 packets.

To estimate the wide bandwidth CIR, spectrum splicing is applied on the collected CFR samples over all and half of the sub-bands. The results are presented in Figures 5 and 6, respectively. The plots depict the estimated two strongest paths for different sub-channel width (illustrated by the markers), compared towards the 80 MHz CIR. In all cases the method correctly compute the strongest 80 MHz paths in terms of delay.

However, differently from simulations, the amplitude of the CIR slightly fluctuates over the collected packets at each band as a consequence of the dynamic environment, even though the transmitter and the receiver are static. This slight fluctuation impacts the OMP algorithm on delay estimation.

Therefore, to study the algorithm performance, we collected 100 packets and computed the ecdf for the estimated two strongest paths for the 100 packets, over all and 50% 20 MHz sub-bands. The ground truth are the two 80 MHz peaks delay, respectively, 0 ns and 12.5 ns. The results are given in Figure 7 and show that for such narrow bands, the method sometimes overestimate the delays. Considering that the resolution of the wide band is $1/80 \text{ MHz} = 12.5 \text{ ns}$, the first path is sometimes overestimated up to 2 samples, whereas the second path up to 3 samples. As a future work, we aim to optimize the method, such that the impact of the amplitude variation is ignored.

V. CONCLUSION

Following the key concepts of joint communication and sensing, we realized an OFDM-based channel sounder using spectrum splicing. Spectrum splicing allows to use measurements of multiple narrow-band subchannels to obtain precise wideband measurements. In particular, we validated the low-complexity grid-based spectrum splicing algorithm in simulations and real-world-scenario – making it feasible for internet of things (IoT) solutions. The algorithm is integrated into an IEEE 802.11ac based communication system, where CIR and CFR are estimated using the LS estimation technique. For indoor lab experiments, we implemented the system using an USRP-based SDR. We were particularly interested in the ability to obtain wideband channel properties using only a subset of the narrow-band subchannels. Our system allows a very good estimation of the multipath components in terms of time delay both in simulation as well as in indoor experiments.

We see this work as a first step towards measurements of even wider band channels in the mmWave bands. In future work, we plan further experiments also covering longer distances and more dynamic scenarios. In addition, we aim to analyze the algorithm performance in computing the amplitude for the estimated multi-path components.

REFERENCES

- [1] J. Wang, N. Varshney, C. Gentile, S. Blandino, J. Chuang, and N. Golmie, "Integrated Sensing and Communication: Enabling Techniques, Applications, Tools and Datasets, Standardization, and Future Directions," *IEEE Internet of Things Journal*, Jul. 2022.
- [2] J. A. Zhang, M. L. Rahman, K. Wu, X. Huang, Y. J. Guo, S. Chen, and J. Yuan, "Enabling Joint Communication and Radar Sensing in Mobile Networks - A Survey," *IEEE Communications Surveys & Tutorials*, vol. 24, no. 1, pp. 306–345, 2022.
- [3] T. Wild, V. Braun, and H. Viswanathan, "Joint Design of Communication and Sensing for Beyond 5G and 6G Systems," *IEEE Access*, vol. 9, Jan. 2021.
- [4] Y. Cui, F. Liu, X. Jing, and J. Mu, "Integrating Sensing and Communications for Ubiquitous IoT: Applications, Trends, and Challenges," *IEEE Network*, vol. 35, no. 5, pp. 158–167, Sep. 2021.
- [5] K. Wu, J. A. Zhang, X. Huang, and Y. J. Guo, "OTFS-Based Joint Communication and Sensing for Future Industrial IoT," *IEEE Internet of Things Journal*, vol. 10, no. 3, Feb. 2023.
- [6] S. D. Liyanarachchi, C. B. Barneto, T. Riihonen, and M. Valkama, "Joint OFDM Waveform Design for Communications and Sensing Convergence," in *IEEE International Conference on Communications (ICC 2020)*, Virtual Conference: IEEE, Jun. 2020.
- [7] D. Vasisht, S. Kumar, and D. Katabi, "Decimeter-level localization with a single WiFi access point," in *13th USENIX Symposium on Networked Systems Design and Implementation (NSDI 2016)*, Santa Clara, CA, Mar. 2016, pp. 165–178.
- [8] M. B. Khalilsarai, B. Gross, S. Stefanatos, G. Wunder, and G. Caire, "WiFi-Based Channel Impulse Response Estimation and Localization via Multi-Band Splicing," arXiv, cs.IT 2011.10402, Nov. 2020.
- [9] Y. Wan, A. Liu, R. Du, and T. X. Han, "Fundamental Limits and Optimization of Multiband Sensing," arXiv, eess.SP, Jul. 2022.
- [10] T. Kazaz, G. J. Janssen, J. Romme, and A.-J. Van der Veen, "Delay estimation for ranging and localization using multiband channel state information," *IEEE Transactions on Wireless Communications (TWC)*, vol. 21, no. 4, pp. 2591–2607, 2021.
- [11] Y. Xie, Z. Li, and M. Li, "Precise Power Delay Profiling with Commodity Wi-Fi," *IEEE Transactions on Mobile Computing (TMC)*, vol. 18, no. 6, pp. 1342–1355, Jun. 2019.
- [12] X. Shen, L. Guo, Z. Lu, X. Wen, and Z. He, "WiRIM: Resolution improving mechanism for human sensing with commodity Wi-Fi," *IEEE Access*, vol. 7, pp. 168 357–168 370, Nov. 2019.
- [13] Y. Wan, A. Liu, Q. Hu, M. Zhang, and Y. Cai, "Multiband Delay Estimation for Localization Using a Two-Stage Global Estimation Scheme," arXiv, eess.SP, Jun. 2022.
- [14] T. S. Rappaport, *Wireless Communications: Principles and Practice*. Upper Saddle River, NJ: Prentice Hall, 1996.
- [15] J. Heiskala and J. Terry, *OFDM Wireless LANs: A Theoretical and Practical Guide*. Indianapolis, IN: SAMS, 2001.
- [16] R. Sun, P. B. Papazian, J. Senic, Y. Lo, J.-K. Choi, K. A. Remley, and C. Gentile, "Design and calibration of a double-directional 60 GHz channel sounder for multipath component tracking," in *11th European Conference on Antennas and Propagation (EUCAP 2017)*, Paris, France: IEEE, Mar. 2017, pp. 3336–3340.
- [17] C. Lv, J.-C. Lin, and Z. Yang, "Channel prediction for millimeter wave MIMO-OFDM communications in rapidly time-varying frequency-selective fading channels," *IEEE Access*, pp. 15 183–15 195, Jan. 2019.
- [18] A. Le Ha, T. Van Chien, T. H. Nguyen, W. Choi, and V. Duc Nguyen, "Deep Learning-Aided 5G Channel Estimation," in *15th International Conference on Ubiquitous Information Management and Communication (IMCOM 2021)*, Seoul, South Korea: IEEE, Jan. 2021, pp. 1–7.
- [19] J. A. Tropp and A. C. Gilbert, "Signal recovery from random measurements via orthogonal matching pursuit," *IEEE Transactions on Information Theory*, vol. 53, no. 12, pp. 4655–4666, 2007.